Dalton Transactions

Incorporation of Coinage Metal-NHC Complexes into Heptaphosphide Clusters

Journal:	*Dalton Transactions*
Manuscript ID	DT-COM-09-2020-003119
Article Type:	Communication
Date Submitted by the Author:	06-Sep-2020
Complete List of Authors:	Jo, Minyoung; Florida State University, Department of Chemistry Li, Jingbai; Illinois Institute of Technology, Department of Chemistry Dragulescu-Andrasi, Alina; Florida State University, Department of Chemistry Rogachev, Andrey; Illinois Institute of Technology, Chemistry Shatruk, Michael; Florida State University, Department of Chemistry

COMMUNICATION

Incorporation of Coinage Metal-NHC Complexes into Heptaphosphide Clusters

Received 00th January 20xx,
Accepted 00th January 20xx

DOI: 10.1039/x0xx00000x

Minyoung Jo,[a] Jingbai Li,[b] Alina Dragulescu-Andrasi,[a] Andrey Yu. Rogachev*[b] and Michael Shatruk*[a]

Cu(I) and Au(I) ions, capped with an *N*-heterocyclic carbene (NHC), react with $(TMS)_3P_7$ (TMS = trimethyl-silyl) to afford an η^4-coordinated anion $[NHC^{Dipp}Cu\text{-}P_7(TMS)]^-$ and a neutral trinuclear complex $(NHC^{Dipp}Au)_3P_7$. Protecting the P_7 cage with the TMS groups is instrumental in controlling the course of these reactions.

Polyphosphides represent a fascinating group of anionic species with diverse structural motifs, afforded by the propensity of phosphorus atoms to form homonuclear bonds.[1] While the structural chemistry of polyphosphides has been dominated by materials prepared via solid-state synthesis,[1,2] the potential for further expansion of this chemistry via solution protocols remains underexplored. The Baudler group pioneered research into soluble polyphosphides 1970-80s.[3] Recently, however, a renaissance in the solution chemistry of polyphosphides has been driven by the interest in using them as ligands and building blocks for assembly of larger supramolecular structures.[4-7]

Despite the growth in the number of known structures that contain polyphosphide fragments, it is challenging to control reactivity of these highly fluxional anionic cages that are also air- and moisture-sensitive. Soluble polyanions P_5^-, P_7^{3-}, P_{14}^{4-}, P_{16}^{2-}, P_{21}^{3-}, and P_{26}^{4-} have been established,[3,8-13] but only P_7^{3-} has been functionalized via alkylation,[14-17] protonation,[18,19] and metalation.[20-26] Similar reactions with other polyphosphides are lacking, except for a single report on the alkylation of P_{16}^{2-}.[27] Thus, it is desirable to devise new reaction pathways to expand the solution chemistry of these structurally diverse anions.

The P_7^{3-} anion exhibits high basicity and nucleophilicity due to three formal negative charges localized on the two-bonded phosphorus atoms (Scheme 1).[6] A number of complexes with the P_7^{3-} anion have been reported, with the cage coordinated to the metal center in η^1, η^2, or η^4 fashion (Scheme 1).[20-26] The η^1- and η^2-coordination preserve the nortricyclane structure,

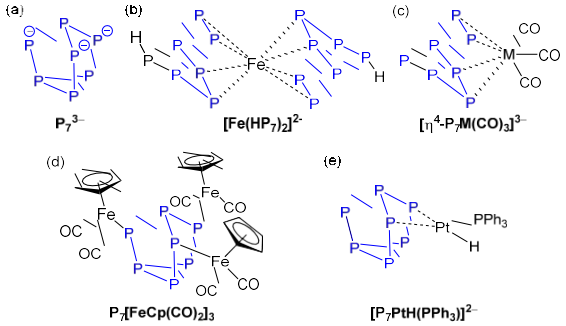

Scheme 1 Typical coordination modes of the P_7^{3-} anion.

but the η^4-coordination generally leads to partial disruption of the P–P bonds. Many such reactions, especially with transition metal ions, are difficult to control due to decomposition of the polyphosphide or fast precipitation of amorphous products.

A possible approach to improve the control over the reactivity of the P_7^{3-} cage is to protect its two-bonded P atoms. For example, a few reports showed an improved stability of a functionalized cage, $(TMS)_3P_7$ (TMS = trimethylsilyl).[28-32] Reactions of $(TMS)_3P_7$ with MCp*-containing precursors (M = Fe, Co) led to the disruption of the P_7-based structure and insertion of metals in the P–P bonds,[25] while reactions with triphos-M (triphos = 1,1,1- tris(diphenylphosphinomethyl)-ethane; M = Co, Ni) also disrupted the cage and yielded a metal-coordinated cyclic triphosphirene unit.[33]

The disruption of the nortricyclane cage in the reactions of $(TMS)_3P_7$ with Fe-, Co-, and Ni-containing precursors might be a result of the stronger bonding between the open-shell metal cations and the phosphorus atoms. Using a weaker bonding, closed-shell d^{10} transition metal ion, capped with a stable co-ligand, might help preserve the structural integrity of the P_7 cage. Metal complexes with *N*-heterocyclic carbenes (NHCs) have been studied as catalysts in many organic reactions, which are typically initiated by a simple salt metathesis.[34-36] We envisaged that a reaction between NHC-MCl (M = Cu, Au) and $(TMS)_3P_7$ should lead to a similar metathesis, resulting in elimination of the chloride and the formation of M–P bonds. A

[a] *Department of Chemistry and Biochemistry, Florida State University, Tallahassee, FL 32306, United States. E-mail: mshatruk@fsu.edu*
[b] *Department of Cnmhemistry, Illinois Institute of Technology, 3101 South Dearborn St, Chicago, IL 60616, United States. E-mail: arogache@iit.edu*
Electronic Supplementary Information (ESI) available: [details of any supplementary information available should be included here]. See DOI: 10.1039/x0xx00000x

precedent for such bonding was offered by coordination of the NHC-M fragments to the white phosphorus molecule, P_4.[37]

The challenge of taming polyphosphides as synthons or ligands is heightened by the limited commercial availability of white phosphorus, commonly considered as a more reactive form of the element, better suited for solution chemistry. In this vein, our group has recently reported a breakthrough in the access to polyphosphides in solution by nucleophilic activation of shelf-stable red phosphorus in non-protic solvents.[38, 39] In the present work, we solubilized red phosphorus by treating it with Na in refluxing tetrahydrofuran (THF). The solid Na_3P_7 that formed after 24 h was redissolved in dimethoxyethane (DME) and treated with (TMS)Cl to obtain a TMS-protected structure (Scheme S1), with the goal to stabilize the P_7^{3-} anion against disruption under action of transition metal ions. The $^{31}P\{^1H\}$ NMR spectrum of the product showed three resonances that matched the chemical shifts reported for $(TMS)_3P_7$ (Fig. 1a).[31]

The reaction of $(TMS)_3P_7$ with $NHC^{Dipp}CuCl$ in THF at room temperature was monitored by ^{31}P NMR spectroscopy, showing a gradual consumption of the heptaphosphide precursor as the amount of $NHC^{Dipp}CuCl$ increased (Fig. 1). A pure intermediate product was observed at the $(TMS)_3P_7$:$NHC^{Dipp}CuCl$ = 1:0.7 ratio (Fig. 1c), while a new product began to form as the amount of $NHC^{Dipp}CuCl$ further increased. Finally, at the 1:3 ratio of starting materials, only a pure second product was observed (Fig. 1f).

The dark-red solution obtained in the end was used to crystallize the final product. The single-crystal X-ray diffraction revealed the crystal structure of complex **1**, [NHC^{Dipp}-Cu-NHC^{Dipp}]$^+$[NHC^{Dipp}Cu-P_7(TMS)]$^-$. Thus, instead of the envisioned trinuclear complex, in which all TMS groups would have been replaced by the NHC-Cu(I) units, we observed the formation of a compound containing both a complex cation and a complex anion. The 1:3 ratio of $(TMS)_3P_7$ to $NHC^{Dipp}CuCl$ required to complete the reaction is justified by the ratio of P_7 to NHC^{Dipp} in the structure of **1**. Obviously, 1/3 of the Cu(I) ions are lost to the CuCl byproduct, which precipiates in the course of the reaciton:

$$(TMS)_3P_7 + 3\ NHC^{Dipp}CuCl \rightarrow 2\ (TMS)Cl + CuCl + [NHC^{Dipp}\text{-}Cu\text{-}NHC^{Dipp}][NHC^{Dipp}Cu\text{-}P_7(TMS)] \quad (\mathbf{1})$$

The structure of **1** contains a $(TMS)P_7^{2-}$ cluster bound to the Cu(I) centre in the η^4-fashion (Fig. 2). Such coordination mode of phosphorus clusters is generally favoured for early transition metals and accompanied by a distortion of the polyphosphide cage and cleavage of a P–P bond. Such situation is observed, for example, in $[Fe(HP_7)_2]^{2-}$ (Scheme 1b)[21] and $[\eta^4\text{-}P_7Cr(CO)_3]^{3-}$ (Scheme 1c).[26] In contrast, late transition metals tend to engage in η^2-coordination with P_7^{3-}, without a significant distortion of the polyphosphide anion (e.g., $[P_7PtH(PPh_3)_2]^{2-}$ in Scheme 1e[40]).

Despite the η^4-coordination of P_7^{3-} to the Cu(I) centre in **1**, we do not observe any dramatic distortion or cleavage of the P–P bonds. The bonds in the basal triangle (Fig. 2) do not form an equilateral triangular, in contrast to the structure of $(TMS)_3P_7$ with nearly identical basal P–P bonds (2.213-2.215 Å).[41] We attribute this rather weak distortion of the basal triangle to the softer nature of interaction between P_7^{3-} and the closed-shell Cu(I) ion. The Cu–P bonds are longer as compared to 2.307 Å in $P_4CuGaCl_4$[42] or the range of 2.336-2.342 Å in $[Cu(P_4)_2]^+$,[43] in both

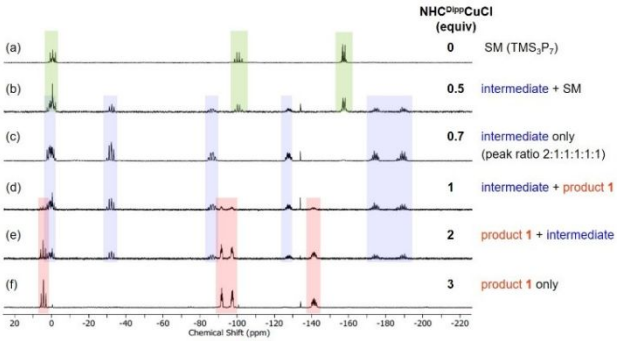

Fig. 1 ^{31}P-NMR spectra monitoring progress of the reaction between $(TMS)_3P_7$ and $NHC^{Dipp}CuCl$ vs. the stoichiometry.

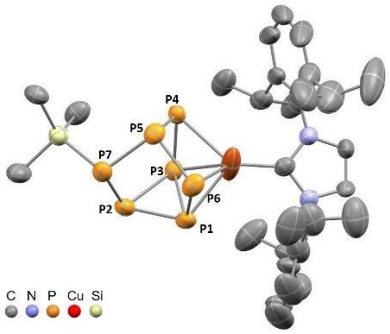

Fig. 2 The [$NHC^{Dipp}Cu(\eta^4\text{-}P_7)$(TMS)]$^-$ anion in the structure of **1**. Thermal ellipsoids are shown at 50% probability level. The counter-ion and hydrogen atoms are omitted for clarity. The full asymmetric unit is shown in Fig. S1. Selected bond lengths (Å): Cu–P6, 2.366(3); Cu–P1, 2.416(3); Cu–P3, 2.470(4); Cu–P4, 2.482(4) Å; P1–P2, 2.204(5); P2–P3, 2.254(5), P1–P3, 2.368(5).

of which the Cu(I) ion exhibits η^2-coordination to the P_4 molecule. The longer Cu–P distances in **1** can be attributed both to the larger coordination number of Cu(I) and to the bulkiness of the NHC ligand. In turn, the Cu–C distance to the carbene decreased from 1.953 Å in $NHC^{Dipp}CuCl$[44] to 1.907(7) Å in **1**.

The nature of bonding was studied with DFT calculations. The fully-relaxed optimized geometry of [$NHC^{Dipp}Cu\text{-}P_7$(TMS)]$^-$ converged to an η^2-coordination (Fig. S16a), which is different from the crystal structure. Therefore, we used the experimental geometry, in which only H atoms were optimized. The total bonding energy is equal to –88.83 kcal/mol, including –150.03 kcal/mol of the total interaction energy (ΔE_{int}) between $(TMS)P_7^{2-}$and [NHC^{Dipp}-Cu(I)]$^+$ and +61.20 kcal/mol of the preparation energy (ΔE_{prep}). The latter describes changes in geometry of interacting fragments upon going from isolated species to components of the aggregate. Energy decomposition analysis (EDA)[45,46] was used to quantify attractive electrostatic (ΔE_{elstat}), orbital (ΔE_{orb}), and repulsive Pauli (ΔE_{Pauli}) bonding components, which were equal to –262.78, –57.61, and +170.35 kcal/mol, respectively. The Natural Bond Orbital analysis[47] was used to quantify contributions from different P atoms. The $(TMS)P_7^{2-}$ revealed notable donor behavior of P1, P3, P4, and P6 atoms through the 3*s* and 3*p* orbitals that interact with the acceptor 4*s* orbital of Cu(I), to give a total stabilization energy of 201.78 kcal/mol (Table S2 and Fig. S17). The 3*p*(P4) → 4*s*(Cu)

and 3*p*(P6) → 4*s*(Cu) interactions are the strongest (51.56 and 64.64 kcal/mol, respectively), which might explain why the DFT optimization converged to the η²-coordination. Weak π-back-donation occurs from the 3*d* orbital of Cu(I) to the P1–P3 σ*-orbital (6.66 kcal/mol), which agrees with the shortened Cu–C distance in the crystal structure of **1**. Analysis of electron density by means of Quantum Theory of Atoms In Molecules[48] revealed only three bond critical points (BCPs) formed between the P3, P4, and P6 atoms and Cu (Fig. S18). The lack of a BCP in the Cu–P1 bond can be explained by coalescence of the aimed BCP with another critical point, resulting in a non-nuclear attractor between the P1 and P6 atoms due to the non-optimized geometrical configuration. Thus, the hapticity in the target system is best described as asymmetrical η⁴ coordination.

The $^{31}P\{^{1}H\}$ NMR spectrum of **1** revealed four independent multiplets at 1.8, –89.4, –98.7, and –141.7 ppm, with the 1:2:2:2 intensity ratio (Fig. 1f). The assignment of resonances was aided by analysis of a ^{31}P-^{31}P COSY spectrum (Fig. S2). Compared to the spectrum of $(TMS)_3P_7$, which showed three resonances with an intensity ratio of 3:1:3 (Fig. 1a), the spectrum of **1** reflects the lower symmetry of the η⁴-coordinated P_7. A similar AA´BB´CC´X-type spectrum was observed for $[\eta^4\text{-}HP_7Cr(CO)_3]^{2-}$.[23]

Neither the calculated nor the crystal structure geometry of the $[NHC^{Dipp}Cu\text{-}P_7(TMS)]^-$ anion allowed us to reproduce the experimental ^{31}P-NMR spectrum of **1**. The DFT-optimized geometry, with or without implicit solvent, showed an η²-coordination, which may explain the disagreement between the calculated and experimental chemical shifts (Fig. S16). Although the crystal structure has an asymmetric η⁴-coordination, we hypothesize that the solution structure undergoes dynamic changes in the η⁴-coordination, most likely, balancing between two extremes of the η²-coordination of the Cu(I) center to the P1-P3-P4-P6 face. This hypothesis is supported by the observation of two disordered components of the η⁴-coordinated P_7 cage in the crystal structure of **1** (Fig. S1b).

As mentioned above, an intermediate product was observed in the reaction as the $(TMS)_3P_7$ to $NHC^{Dipp}CuCl$ ratio changed from 1:0.5 to 1:3 (Fig. 1). The ^{31}P-NMR spectrum of the intermediate showed six resonances in the 2:1:1:1:1:1 intensity ratio, which might correspond to the initial substitution of one TMS group by $NHC^{Dipp}Cu^+$. To verify this hypothesis, we carried out DFT calculations on the structure of $[NHC^{Dipp}Cu\text{-}P_7(TMS)_2]$. The geometry optimization yielded a linearly coordinated Cu(I) complex (Fig. 3a), the ^{31}P-NMR spectrum of which is in excellent agreement with the spectrum of the intermediate (Fig. 3b).

Seeking to substitute all three TMS groups, we reacted the $(TMS)_3P_7$ cluster with a NHC-gold precursor, keeping in mind the strong preference of Au(I) for linear coordination. Treatment of $(TMS)_3P_7$ with $NHC^{Dipp}AuCl$ in THF in a 1:3 stoichiometric ratio led to the substitution of all three TMS groups by $NHC^{Dipp}Au^+$ units to afford a neutral trinuclear complex:

$$(TMS)_3P_7 + 3\ NHC^{Dipp}AuCl \rightarrow 3\ (TMS)Cl + (NHC^{Dipp}Au)_3P_7\ (\mathbf{2})$$

A similar example is offered by $P_7[FeCp(CO)_2]_3$,[25] which, to the best of our knowledge, is the only other reported case of the three-fold coordination of transition metals to the P_7 cage. The linear coordination of the Au(I) ions, the bulky capping ligands,

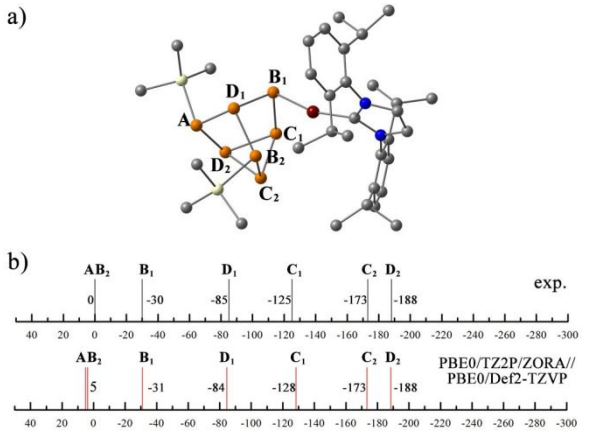

Fig. 3 (a) The proposed DFT-optimized structure of the intermediate observed in the reaction between $(TMS)_3P_7$ and $NHC^{Dipp}CuCl$. The H atoms are omitted for clarity. (b) The experimental $^{31}P\{^{1}H\}$ NMR chemical shifts observed at the 1:0.7 ratio of the reactants and the calculated chemical shifts.

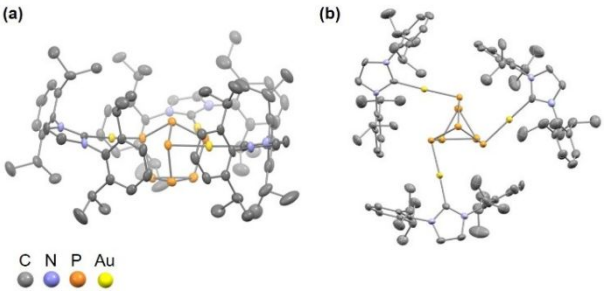

Fig. 4 Side (a) and top (b) views of the crystal structure of **2**. Thermal ellipsoids are shown at 50% probability level.

and the approximate axial C_{3v} symmetry of the P_7 cage impart chirality to complex **2**. The crystal structure, however, is centrosymmetric, since the unit cell contains equal numbers of stereoisomers with the opposite chirality (Fig. S1c).

The shape of the original seven-atom cage in **1** is essentially preserved, and the coordination of three $NHC^{Dipp}Au^+$ units only causes minor perturbations to the cage geometry (Fig. 4). The P–P bond lengths vary from 2.179(1) to 2.233(1) Å, being only marginally longer than those in $(TMS)_3P_7$ (2.178–2.215 Å). The Au–P bond distances of 2.314(1), 2.319(1), and 2.342(1) Å are shorter than the Au–P bonds observed in related complexes, i.e. 2.357 and 2.349 Å in $[Au_2(HP_7)_2]^{2-}$,[20] and 2.404 and 2.428 Å in $[NHC^{Dipp}Au(\eta^2\text{-}P_4)]^+$.[37] The Au–C bond, however, is lengthened from 1.998 Å in $NHC^{Dipp}AuCl$[49] to 2.033(4)–2.053(4) Å in **2**, likely due to steric congestion from the NHC ligands.

The $^{31}P\{^{1}H\}$ NMR spectrum of **2** exhibits three resonances with an intensity ratio of 3:1:3 (Fig. S13). The spectrum is thus very similar to the one observed for the $(TMS)_3P_7$ precursor. A notable difference between the spectra is the shift of all three multiplets (Fig. S19). The peaks at 0 and –99.8 ppm, assigned, respectively, to the substituted P atoms (A) and the apex P atom (B) in $(TMS)_3P_7$, have been shifted downfield to 8.9 and –79.5 ppm in the spectrum of **2**, while the peak at –156.8 ppm, due to the basal P atoms (C) in $(TMS)_3P_7$, is shifted to –183.5 ppm in **2**.

The DFT-optimized geometry of complex **2** agrees well with the crystal structure. The computed Au–P bonds of 2.352 Å, 2.354 Å, and 2.357 Å are slightly longer than the experimental values. The P–P bond lengths range from 2.189 Å to 2.227 Å, also in accord with the experimental structure. The calculated ^{31}P-NMR spectra of $(TMS)_3P_7$ and **2** show an excelent agreement with the exerimental spectra (Fig. S19).

In summary, the use of TMS-protected P_7 cage has afforded better control over its reactions with NHC-d[10] metal complexes, yielding the anionic $[(NHC^{Dipp}Cu)\eta^4\text{-}P_7(TMS)]^-$ and the neutral $(NHC^{Dipp}Au)_3P_7$ with unique molecular structures. Although two isoelectronic coinage metal ions give rise to different binding modes toward the P_7^{3-} cage, this difference is well justified by established coordination preferences of the Cu(I) and Au(I) ions. We also highlight that our facile synthetic route to produce soluble polyphosphides[38,39] should allow further expansion of studies on the solution reactivity of these fascinating species, thus opening possibilities for a wide variety of modifications of the phosphorus-rich molecules with different functionalities.

Conflicts of interest

There are no conflicts to declare.

Acknowledgements

This work was supported by the U.S. Department of Defense (award DOTC 13-01-INIT518) and in part by the National Science Foundation (award CHE-1955754).

1 R. Pöttgen, W. Hönle and H. G. von Schnering, in *Encyclopedia of Inorganic Chemistry*, ed. R. B. King, Wiley, Chichester, 2005, vol. 8, pp. 4255-4308.
2 M. Shatruk, in *Fundamentals and Applications of Phosphorus Nanomaterials*, American Chemical Society, Washington, DC, 2019, vol. 1333, pp. 103-134.
3 M. Baudler, *Angew. Chem. Int. Ed. Engl.*, 1987, **26**, 419-441.
4 M. Scheer, G. Balazs and A. Seitz, *Chem. Rev.*, 2010, **110**, 4236-4256.
5 M. Caporali, L. Gonsalvi, A. Rossin and M. Peruzzini, *Chem. Rev.*, 2010, **110**, 4178-4235.
6 R. S. P. Turbervill and J. M. Goicoechea, *Chem. Rev.*, 2014, **114**, 10807-10828.
7 B. M. Cossairt, N. A. Piro and C. C. Cummins, *Chem. Rev.*, 2010, **110**, 4164-4177.
8 M. Baudler, *Angew. Chem. Int. Ed. Engl.*, 1982, **21**, 492-512.
9 H. G. von Schnering, V. Manriquez and W. Hönle, *Angew. Chem. Int. Ed. Engl.*, 1981, **20**, 594-595.
10 M. Baudler, D. Düster, K. Langerbeins and J. Germeshausen, *Angew. Chem. Int. Ed. Engl.*, 1984, **23**, 317-318.
11 M. Baudler, R. Heumüller, D. Düster, J. Germeshausen and J. Hahn, *Z. Anorg. Allg. Chem.*, 1984, **518**, 7-13.
12 M. Baudler, S. Akpapoglou, D. Ouzounis, F. Wasgestian, B. Meinigke, H. Budzikiewicz and H. Münster, *Angew. Chem. Int. Ed. Engl.*, 1988, **27**, 280-281.
13 F. Guerin and D. Richeson, *Inorg. Chem.*, 1995, **34**, 2793-2794.
14 R. S. P. Turbervill and J. M. Goicoechea, *Organometallics*, 2012, **31**, 2452-2462.
15 V. A. Milyukov, A. V. Kataev, E. Hey-Hawkins and O. G. Sinyashin, *Russ. Chem. Bull.*, 2007, **56**, 298-303.
16 S. Charles, J. C. Fettinger and B. W. Eichhron, *J. Am. Chem. Soc.*, 1995, **117**, 5303-5311.
17 M. Baudler, W. Faber and J. Hahn, *Z. Anorg. Allg. Chem.*, 1980, **469**, 15-21.
18 F.-R. Dai and L. Xu, *Inorg. Chim. Acta*, 2006, **359**, 4265-4273.
19 M. Baudler and K. Glinka, *Chem. Rev.*, 1993, **93**, 1623-1667.
20 C. M. Knapp, C. S. Jackson, J. S. Large, A. L. Thompson and J. M. Goicoechea, *Inorg. Chem.*, 2011, **50**, 4021-4028.
21 C. M. Knapp, J. S. Large, N. H. Rees and J. M. Goicoechea, *Chem. Commun.*, 2011, **47**, 4111-4113.
22 C. Knapp, B. Zhou, M. S. Denning, N. H. Rees and J. M. Goicoechea, *Dalton Trans.*, 2010, **39**, 426-436.
23 S. Charles, J. C. Fettinger, S. G. Bott and B. W. Eichhorn, *J. Am. Chem. Soc.*, 1996, **118**, 4713-4714.
24 S. Charles, J. C. Fettinger and B. W. Eichhorn, *Inorg. Chem.*, 1996, **35**, 1540-1548.
25 R. Ahlrichs, D. Fenske, K. Fromm, H. Krautscheid, U. Krautscheid and O. Treutler, *Chem. Eur. J.*, 1996, **2**, 238-244.
26 S. Charles, B. W. Eichhorn, A. L. Rheingold and S. G. Bott, *J. Am. Chem. Soc.*, 1994, **116**, 8077-8086.
27 M. Baudler and R. Becher, *Z. Naturforsch. B*, 1985, **40**, 1090-1092.
28 M. Cicač-Hudi, J. Bender, S. H. Schlindwein, M. Bispinghoff, M. Nieger, H. Grützmacher and D. Gudat, *Eur. J. Inorg. Chem.*, 2016, 649-658.
29 G. Fritz and J. Härer, *Z. Anorg. Allg. Chem.*, 1983, **504**, 23-37.
30 G. Fritz, K. D. Hoppe, W. Hönle, D. Weber, C. Mujica, V. Manriquez and H. G. von Schnering, *J. Organomet. Chem.*, 1983, **249**, 63-80.
31 G. Fritz and W. Hölderich, *Naturwiss.*, 1975, **62**, 573-575.
32 P. Noblet, A. Dransfeld, R. Fischer, M. Flock and K. Hassler, *J. Organomet. Chem.*, 2011, **696**, 652-660.
33 M. Peruzzini and P. Stoppioni, *J. Organomet. Chem.*, 1985, **288**, c44-c46.
34 Y. Shido, M. Yoshida, M. Tanabe, H. Ohmiya and M. Sawamura, *J. Am. Chem. Soc.*, 2012, **134**, 18573-18576.
35 H. Wu, J. M. Garcia, F. Haeffner, S. Radomkit, A. R. Zhugralin and A. H. Hoveyda, *J. Am. Chem. Soc.*, 2015, **137**, 10585-10602.
36 M. Jo, D. Rivalti, A. R. Ehle, A. Dragulescu-Andrasi, M. Hartweg, M. Shatruk and D. T. McQuade, *Synlett*, 2018, **29**, 2673-2678.
37 J. E. Borger, M. S. Bakker, A. W. Ehlers, M. Lutz, J. Chris Slootweg and K. Lammertsma, *Chem. Commun.*, 2016, **52**, 3284-3287.
38 A. Dragulescu-Andrasi, L. Z. Miller, B. Chen, D. T. McQuade and M. Shatruk, *Angew. Chem. Int. Ed.*, 2016, **55**, 3904-3908.
39 M. Jo, A. Dragulescu-Andrasi, L. Z. Miller, C. Pak and M. Shatruk, *Inorg. Chem.*, 2020, **59**, 5483-5489.
40 B. Kesanli, S. Charles, Y. F. Lam, S. G. Bott, J. Fettinger and B. Eichhorn, *J. Am. Chem. Soc.*, 2000, **122**, 11101-11107.
41 W. Hönle and H. G. von Schnering, *Z. Anorg. Allg. Chem.*, 1978, **440**, 171-182.
42 L. C. Forfar, T. J. Clark, M. Green, S. M. Mansell, C. A. Russell, R. A. Sanguramath and J. M. Slattery, *Chem. Commun.*, 2012, **48**, 1970-1972.
43 G. Santiso-Quinones, A. Reisinger, J. Slattery and I. Krossing, *Chem. Commun.*, 2007, 5046-5048.
44 H. Kaur, F. K. Zinn, E. D. Stevens and S. P. Nolan, *Organometallics*, 2004, **23**, 1157-1160.
45 K. Morokuma, *J. Chem. Phys.*, 1971, **55**, 1236-1244.
46 T. Ziegler and A. Rauk, *Inorg. Chem.*, 1979, **18**, 1755-1759.
47 A. E. Reed, L. A. Curtiss and F. Weinhold, *Chem. Rev.*, 1988, **88**, 899-926.
48 R. F. W. Bader, *Atoms in Molecules: A Quantum Theory*, Clarendon Press, Oxford, 1994.
49 A. Linden, T. d. Haro and C. Nevado, *Acta Crystallogr. Sect. C*, 2012, **68**, m1-m3.

A Me_3Si-protected P_7 cage reacts with *N*-heterocyclic-carbene complexes of coinage metals to yield a mononuclear Cu(I) complex featuring a Cu(η^4-P_7) core and a trinuclear Au(I) complex with linearly coordinated metal ions attached to the P_7 cluster.